# On-chip Detection from Directly Modulated Quantum Dot Microring Lasers on Si

**Yating Wan**[1], **Daehwan Jung**[1], **Daisuke Inoue**[1, 2], **Justin C. Norman**[3], **Chen Shang**[3], **Arthur C. Gossard**[3, 4], **and John E. Bowers**[3, 4]

[1]Institute for Energy Efficiency, University of California Santa Barbara
Santa Barbara, California 93106, USA
[2]Institute of Innovative Research, Tokyo Institute of Technology, Tokyo 152-8552, Japan
[3]Materials Department, University of California Santa Barbara, Santa Barbara, California 93106, USA
[4]Department of Electrical and Computer Engineering, University of California Santa Barbara
Santa Barbara, California 93106, USA

**Abstract**— We present on-chip detection from directly modulated microring quantum-dot (QD) lasers grown on exact (001) Si. Static and dynamic properties of the QD-based microring lasers and microdetectors have been investigated. The ring lasers exhibit high temperature stabilities up to 100°C, low thresholds down to sub milliamp, and a wide 3 dB bandwidth up to 6.5 GHz. The microdetectors show small dark currents down to 0.2 nA and eye openings up to 10 Gbit/s with non-return-to-zero signals. Light emission from the microring lasers can be probed via the changes in the photocurrent of the microdetectors, realizing on-chip QD laser and detector system on Si by epitaxy. Furthermore, demonstrated downscaling abilities of the QD based devices promise improved integration density for photonic integrated circuits (PIC).

## 1. INTRODUCTION

Harnessing quantum dots (QDs) with micro-cavities promises to meet the demands for low-power consumption, and small-footprint optical interconnect systems in silicon-based microelectronic chips [1–3]. By virtue of the in-plane carrier confinement properties of QDs to combat heteroepitaxial defects, the performance of monolithically grown lasers on Si is improving rapidly [4–7]. Continuous-wave (CW) threshold currents below 1 mA [8], injection efficiencies of 87%, output powers of 175 mW at 20°C [9], and 4000-h reliability tests at 35°C with an extrapolated mean-time-to-failure of more than ten million hours [10] have been demonstrated. The overall performances of these devices are comparable to or outperform those achieved by heterogeneous integration, while offering substantial manufacturing cost and scalability advantages over their counterparts [2]. To further achieve the goal of attojoule optoelectronics for on-chip interconnects [11], the small-footprint micro-cavity lasers, with their inherent traveling wave operation nature requiring no gratings or Fabry-Perot (FP) facets, are particularly attractive [12].

Here, we present on-chip photo-detection from a monolithically integrated QD microring laser through free-space coupling. The on-chip microdetectors operate with an ultra-low dark current of 0.2 nA in the O band, which corresponds to a small dark current density of 0.13 mA/cm$^2$. High speed measurement shows 3dB bandwidth of 5.5 GHz at a bias voltage of −5 V. Large signal measurement with non-return-to-zero (NRZ) signals exhibits an eye opening at 10 Gbit/s operation. The microring laser possesses a low threshold current of 3 mA under CW electrical injection and sustains lasing at elevated temperatures up to 100°C under pulsed injection. A $T_0$ was extracted to be ∼60 K from 10–80°C, and ∼20 K between 80–100°C. Shrinkage of device dimensions show monotonic decrease of threshold currents. The indicated low impact of sidewall recombination promises further downscaling of devices. This preliminary version of integrating microring lasers with microdetectors on the monolithic device platform shows great potential to realize complex and scalable photonic integrated circuits (PICs) on industry standard silicon substrates.

## 2. EXPERIMENT AND RESULT

The microring lasers and microdetectors were integrated without any additional processing steps as the two devices were fabricated simultaneously on a single active region design. The complete epitaxial structure is shown in Fig. 1(a). The detailed growth procedure on the Si (001) template was reported in [13]. Two GaAs/Al$_x$Ga$_{1-x}$As graded index separate confinement heterostructure (GRINSCH) lasers with seven layers of InAs/InGaAs quantum dot-in-a-well (DWELL) active layers were grown subsequently. A dot density of $5.2 \times 10^{10}$ cm$^{-2}$ was measured using atomic force

© 2018 IEICE

microscopy (AFM) and a strong luminescence at 1285 nm with a full-width at half-maximum of 28 meV was obtained from photoluminescence measurements. From the as-grown materials, ring resonators with varying radii and ring waveguide widths were fabricated for lasers while rectangular shape mesa waveguides were formed for the microdetectors. The etched surface was covered with $Al_2O_3$ by atomic layer deposition (ALD) to suppress surface leakage current. The detailed fabrication after the growth can be found in Ref. [8]. A schematic of the on-chip detection system is presented in the upper inset in Fig. 1(b). The laser is located face-to-face alongside the microdetector, probed on a copper heat sink. Scattering of light from the lasers is free-space coupled to the rectangular-shaped microdetector and probed via the changes in the photocurrent. The photocurrent was measured from the microdetector at a $-3$ V bias, while forward-biasing the micro-ring laser. Fig. 1(b) shows the measured photocurrent as a function of the injection current for a micro-ring laser with a mesa width of 4 μm and an outer-ring radius of 25 μm. The measured photocurrent suggests a low lasing threshold of around 3 mA.

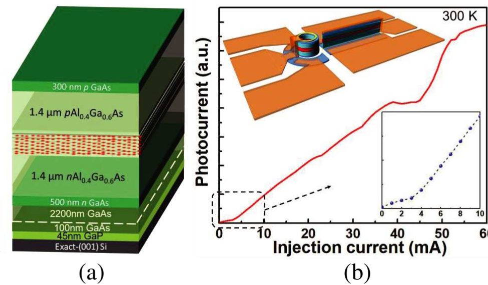


Figure 1: (a) Schematic of the complete epitaxial structure; (b) photocurrent as a function of the injection current for the on-chip micro-ring laser. Inset: schematic of the on-chip detection system.

Temperature dependent characteristics of the micro-ring laser were evaluated separately in a pulse set up with 0.5% duty cycle and 5 μs pulse width. Measured light-current (L-I) curves as a function of the heatsink temperature were analyzed in Fig. 2(a). Lasing behavior was observed up to 100°C, limited by the thermoelectric heater. The blue dots and dashed line in the inset of Fig. 2(a) show the laser threshold versus temperature curve and fitting. An excellent characteristic temperature $T_0$ was extracted to be ∼60 K between 10–80°C, and ∼20 K between 80–100°. Static and dynamic characteristics of the microdetectors were measured by cleaving the diode facet for light input from a lensed fiber. Fig. 2(b) shows current-voltage (I-V) characteristics of $3 \times 50\,\mu m^2$ device without illumination. The dark current was 0.2 nA at a bias voltage of $-3$ V, corresponding to an ultra-low dark current density of 0.13 mA/cm$^2$. This value is two orders of magnitude lower than the competing Ge-on-Si photodiodes with thin Ge or SiGe buffer layers (typically in the order of 10 mA/cm$^2$) [14]. The corresponding wavelength dependence of responsivity of the microdetectors was presented in the inset of Fig. 2(b). A 3 dB coupling loss between the spherical-lensed fiber and the waveguide facet, and ∼30% reflection off the waveguide facet were assumed. Fabry-Perot resonance is occurred between the rear and front facets, and could be further removed using a tilted facet.

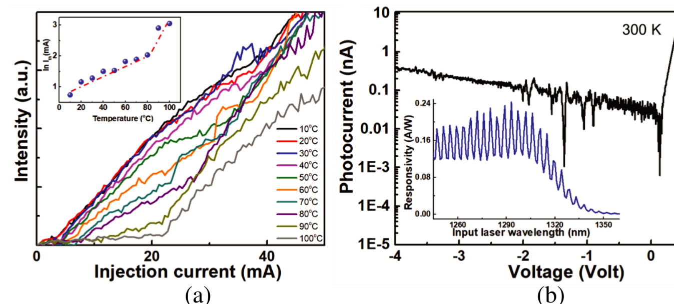


Figure 2: (a) L-I curves as a function of the heatsink temperature. Inset: laser threshold versus temperature curve and fitting. (b) I-V characteristics of the microdetectors without illumination. Inset: wavelength dependence of responsivity.

Small-signal modulation responses $S_{21}$ of the ring laser and microdetector were measured using a

© 2018 IEICE

20 GHz lightwave component analyzer (LCA, HP8703A) and presented in Fig. 3. The devices were directly probed using a signal/ground (SG) RF probe. For the ring laser, injected currents were varied from 21 to 86 mA. These responses are normalized at low-frequency and a 3dB bandwidth of 6.5 GHz was attained at a bias current of 86 mA (Fig. 3(a)). The responses were further fitted using a three-pole fitting function H(f) [15]. The damping rate $\gamma$ and relaxation oscillation frequency $f_\gamma$ at each bias current were extracted. The extracted $f_\gamma$, together with the measured $f_{3\,\mathrm{dB}}$ are plotted in the inset in Fig. 3(a) as a function of the square root of bias current above threshold. The modulation efficiencies of 0.38 GHz/mA$^{1/2}$ for $f_{3\,\mathrm{dB}}$ and 0.34 GHz/mA$^{1/2}$ for $f_\gamma$ were extracted by linear fitting, using the data points below $(I_b I_{th})1/2 = 8\,\mathrm{mA}^{1/2}$. For the microdetector, biased voltages were changed from -1 to -5 V. The maximum 3 dB bandwidth was 5.5 GHz at $-5$ V (Fig. 3(b)). Eye diagram of the microdetector was measured using NRZ signals. A clear eye opening up to data-rate of 10 Gbit/s shown in the inset of Fig. 3(b) is well consistent with the small-signal bandwidth of 5.5 GHz.

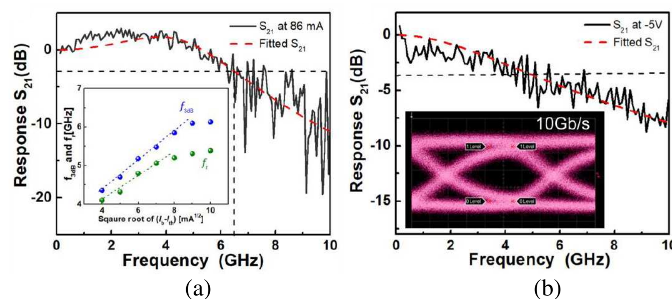


Figure 3: Small-signal modulation response $S_{21}$ of (a) the ring laser and (b) the microdetector. Inset in (a): the extracted $f_\gamma$, and the measured $f_{3\,\mathrm{dB}}$ as a function of the square root of bias current above threshold for the ring laser. Inset in (b): eye opening up to data-rate of 10 Gbit/s for the microdetector.

A summary of the historical trends in CW threshold currents and operating temperatures of QD lasers epitaxially grown on Si is listed in Table 1 and deployed in Fig. 4(a). Competitive work is being conducted in developing CMOS compatible, epitaxial materials platforms on Si, leading to impressive results in material quality and record setting device performance. The benchmarking shows that the micro-ring lasers achieved the smallest footprint, lowest energy consumption, and are tolerant of the highest temperatures sustained near the electronic processors.

Table 1: Historical trends in thresholds and operating temperatures of QD lasers epitaxially grown on Si (R denotes the outer-ring radius, W denotes the ring waveguide width).

| **Year** | **$I_{th}$(mA)/$J_{th}$(A/cm$^2$)** | **Max T (°C)** | **Size (µm$^2$)** | **Laser type** | **Institute** | **$\lambda$ (µm)** | **Ref** |
|---|---|---|---|---|---|---|---|
| **2016** | 100/62.5 (offcut Si) | 75 | 3200×50 | FP(CW) | UCL | 1.32 | [5] |
| **2017** | 32/1066 (on-axis Si) | 90 | 750×4 | FP(CW) | UCSB | 1.28 | [16] |
| **2017** | 187.5/250 (on axis Si) | 36 | 3000×25 | FP(CW) | UCL | 1.29 | [17] |
| **2017** | 36/500 (on-axis Si) | 80 | 1200×6 | FP(CW) | UCSB | 1.25 | [18] |
| **2017** | 15/1200 (on-axis Si) | 100 | R/W=50/4 µm | Ring(CW) | UCSB | 1.3 | [19] |
| | 0.5/995 (on-axis Si) | 100 | R/W=5/3 µm | Ring(CW) | UCSB | 1.3 | [8] |
| **2018** | 3/250 (on-axis Si) | 80 | R/W=15/4 µm | Ring(CW) | UCSB | 1.3 | [13] |
| **2018** | 512/320 (on-axis Si) | 70 | 2000×80 | FP(pulse) | UTokyo | 1.3 | [13] |
| **2018** | 9.5/255 (on-axis Si) | 80 | 1485×2.5 | FP(CW) | UCSB | 1.25 | [20] |
| **2018** | 12/550 (on-axis Si) | 30 | 1000×2.2 | DFB(CW) | UCL | 1.3 | [21] |

The micro-rings in our research group has also undergone several batches of improvements, using different III-V/Si buffer templates with pseudomorphic GaP layers (GaP/Si) [22] and aspect ratio trapping V-grooved trenches (GoVS) [23]. Generation-I (Gen-I) template relies on V-grooved trenches in an on-axis Si substrate to limit defect propagation through aspect ratio trapping, and coalescence of an overgrown GaAs layer to provide bulk area. The Gen-II and Gen-III templates

© 2018 IEICE 

utilized a 45 nm pseudomorphic GaP layer grown directly on Si by metal-organic chemical vapor deposition (MOCVD) that was pioneered by NAsPIII/V, GmbH. For Gen-III, the GaAs barriers separating the quantum dots were partially p-modulation-doped with beryllium. Otherwise, the laser structures of the three batches are nominally the same. Fig. 4(b) summarizes the threshold currents obtained from a series of microring lasers with different outer-ring radii and a constant ring waveguide width of 4 μm from the three batch of lasers. The threshold current was monotonically decreased with the reduction of the ring diameter, and continue the trends even at the smallest dimensions. The demonstrated low impact of sidewall recombination is highly favorable for device miniaturization without imposing a heavy penalty on the threshold current of laser devices.

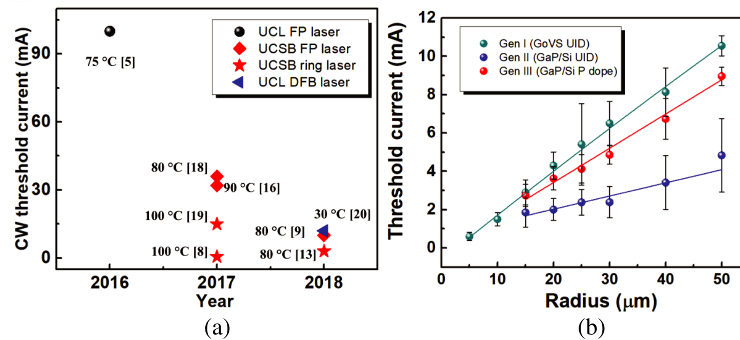


(a) (b)

Figure 4: (a) Historical trends in threshold currents and maximum operating temperatures of QD lasers epitaxially grown on Si. (b) Threshold current for microring lasers grown on Si shows decreasing thresholds as a function of ring radius.

## 3. CONCLUSION

In conclusion, a proof-of-principle demonstration of a low-footprint optical interconnect has been achieved on an industrial-standard Si chip, fabricated through monolithic integration of O-band microring lasers and microdetectors. High temperature stabilities up to 100°C, low thresholds down to sub milliamp, and a wide 3dB bandwidth up to 6.5 GHz have been achieved for the ring lasers. Ultra-low dark currents down to 0.2 nA and eye openings up to 10 Gbit/s with NRZ signals have been achieved for the microdetectors. Optimizing the individual components is expected to further increase link efficiencies and yield a data rate of 10 Gb/s and above. On-chip photodetection from a monolithically integrated QD micro-ring laser through waveguide coupling is also being researched to realize higher efficiency directional emission and detection.

## ACKNOWLEDGMENT

This research was supported by Advanced Research Projects Agency-Energy (ARPA-E) DE-AR000067 and Japan Society for the Promotion of Science (JSPS) Grants-in-Aid for Scientific Research (KAKENHI) (15J11776). We are also grateful to Di liang, Chong Zhang, and Minh Tran for fruitful discussions.

## REFERENCES

1. Ge, L., L. Feng, and H. G. L. Schwefel, "Optical microcavities: New understandings and developments," *Photon. Res.*, Vol. 5, OM1–OM3, 2017.
2. Norman, J., D. Jung, Y. Wan, J. E. Bowers, "Perspective: The future of quantum dot photonic integrated circuits," *APL Photonics*, Vol. 3, 030901, 2018.
3. Bimberg, D. and U. W. Pohl, "Quantum dots: Promises and accomplishments," *Mater. Today*, Vol. 14, No. 9, 388–397, 2011.
4. Zhou, Z., B. Yin, and J. Michel, "On-chip light sources for silicon photonics," *Light Sci. Appl.*, Vol. 4, e358, 2015.
5. Chen, S., W. Li, J. Wu, Q. Jiang, M. Tang, S. Shutts, S. Elliott, A. Sobiesierski, A. Seeds, I. Ross, P. Smowton, and H. Liu, "Electrically pumped continuous-wave III-V quantum dot lasers on silicon," *Nat. Photonics*, Vol. 10, No. 5, 307–311, 2016.

6. Wan, Y., Q. Li, A. Y. Liu, W. W. Chow, A. C. Gossard, J. E. Bowers, E. L. Hu, and K. M. Lau, "Sub-wavelength InAs quantum dot micro-disk lasers epitaxially grown on exact Si (001) substrates," *Appl. Phys. Lett.*, Vol. 108, No. 22, 221101, 2016.
7. Jung, D., Z. Zhang, J. Norman, R. Herrick, M. J. Kennedy, P. Patel, K. Turnlund, C. Jan, Y. Wan, A. C. Gossard, and J. E. Bowers, "Highly reliable low threshold InAs quantum dot lasers on on-axis (001) Si with 87% injection efficiency," *ACS Photonics*, 2017.
8. Wan, Y., J. Norman, Q. Li, M. J. Kennedy, D. Liang, C. Zhang, D. Huang, Z. Zhang, A. Y. Liu, A. Torres, D. Jung, A. C. Gossard, E. L. Hu, K. M. Lau, and J. E. Bowers, "1.3 μm submilliamp threshold quantum dot microlasers on Si," *Optica*, Vol. 4, No. 8, 940–944, 2017.
9. Jung, D., J. Norman, M. J. Kennedy, C. Shang, B. Shin, Y. Wan, A. C. Gossard, and J. E. Bowers, "High efficiency low threshold current 1.3 μm InAs quantum dot lasers on on-axis (001) GaP/Si," *Appl. Phys. Lett.*, Vol. 111, No. 12, 122107, 2017.
10. Jung, D., Z. Zhang, J. Norman, R. Herrick, M. J. Kennedy, P. Patel, K. Turnlund, C. Jan, Y. Wan, A. C. Gossard, and J. E. Bowers, "Highly reliable low threshold InAs quantum dot lasers on on-axis (001) Si with 87% injection efficiency," *ACS Photonics*, 2017.
11. Miller, D. A., "Device requirements for optical interconnects to silicon chips," *Proc. IEEE*, Vol. 97, 1166–1185, 2009.
12. Liang, D., X. Huang, G. Kurczveil, M. Fiorentino, and R. G. Beausoleil, "Integrated finely tunable microring laser on silicon," *Nat. Photonics*, Vol. 10, No. 11, 719–722, 2016.
13. Wan, Y., J. Norman, D. Jung, C. Shang, L. Macfarlane, Q. Li, MJ. Kennedy, Z. Zhang, A. C. Gossard, E. L. Hu, K. M. Lau, and J. E. Bowers, "O-band electrically injected InAs quantum-dot microring lasers on V-groove patterned and unpatterned (001) silicon," *Opt. Express*, Vol. 25, No. 22, 2017.
14. Michel, J., J. Liu, and L. C. Kimerling, "High-performance Ge-on-Si photodetectors," *Nat. Photonics*, Vol. 4, No. 8, 527–534, 2010.
15. Nagarajan, R. L., M. Ishikawa, T. Fukushima, R. S. Geels, and J. E. Bowers, "High speed quantum well lasers and carrier transport effects," *IEEE J. Quantum Electron.*, Vol. 28, No. 10, 1990–2008, 1992.
16. Liu, A. Y., J. Peters, X. Huang, D. Jung, J. Norman, M. L. Lee, A. C. Gossard, and J. E. Bowers, "Electrically pumped continuous-wave 1.3 μm quantum-dot lasers epitaxially grown on on-axis (001) GaP/Si," *Opt. Lett.*, Vol. 42, No. 2, 338–341, 2017.
17. Chen, S., M. Liao, M. Tang, J. Wu, M. Martin, T. Baron, A. Seeds, and H. Liu, "Electrically pumped continuous wave 1.3 μm InAs/GaAs quantum dot lasers monolithically grown on on-axis Si (001) substrates," *Opt. Express*, Vol. 25, No. 5, 4632–4639, 2017.
18. Norman, J., M. J. Kennedy, J. Selvidge, Q. Li, Y. Wan, A. Y. Liu, P. G. Callahan, M. P. Echlin, T. M. Pollock, K. M. Lau, A. C. Gossard, and J. E. Bowers, "Electrically pumped continuous wave quantum dot lasers epitaxially grown on patterned, on-axis (001) Si," *Opt. Express*, Vol. 25, No. 4, 3927–3934, 2017.
19. Wan, Y., J. Norman, Q. Li, M. J. Kennedy, D. Liang, C. Zhang, D. Huang, A. Y. Liu, A. Torres, D. Jung, A. C. Gossard, E. L. Hu, K. M. Lau, and J. E. Bowers, "Sub-mA threshold 1.3 μm CW lasing from electrically pumped micro-rings grown on (001) Si," *CLEO: Applications and Technology*, 2017, paper JTh5C.3.
20. Kwoen, J., B. Jang, L. Joohang, T. Kageyama, K. Watanabe, Y. Arakawa, "All MBE grown InAs/GaAs quantum dot lasers on on-axis Si (001)," *Opt. Express*, Vol. 26, No. 9, 11568–11576, 2018.
21. Wang, Y., S Chen, Y. Yu, L. Zhou, L. Liu, C. Yang, M. Liao, M. Tang, Z. Liu, J. Wu, A. J. Seeds, W. Li, I. Ross, H. Liu, S. Yu, "Electrically-pumped continuous-wave quantum-dot distributed feedback laser array on silicon," arXiv preprint arXiv, 2018.
22. Jung, D., P. G. Callahan, B. Shin, K. Mukherjee, A. C. Gossard, and J. E. Bowers, "Low threading dislocation density GaAs growth on on-axis GaP/Si (001," *J. Appl. Phys.*, Vol. 122, No. 22, 225703, 2017.
23. Li, Q., K. W. Ng, and K. M. Lau, "Growing antiphase-domain-free GaAs thin films out of highly ordered planar nanowire arrays on exact (001) silicon," *Appl. Phys. Lett.*, Vol. 106, No. 7, 072105, 2015.


© 2018 IEICE